

# Double-Walled Carbon Nanotube Solar Cells

Jinquan Wei,<sup>\*,†</sup> Yi Jia,<sup>†</sup> Qinke Shu,<sup>†</sup> Zhiyi Gu,<sup>†</sup> Kunlin Wang,<sup>†</sup> Daming Zhuang,<sup>†</sup> Gong Zhang,<sup>†</sup> Zhicheng Wang,<sup>†</sup> Jianbin Luo,<sup>†</sup> Anyuan Cao,<sup>‡</sup> and Dehai Wu<sup>\*,†</sup>

*Key Lab for Advanced Manufacturing by Materials Processing Technology of Education Ministry, Department of Mechanical Engineering, Tsinghua University, Beijing 100084, China, and Department of Mechanical Engineering, University of Hawaii at Manoa, Honolulu, Hawaii 96822*

Received April 24, 2007; Revised Manuscript Received May 28, 2007

## ABSTRACT

We directly configured double-walled carbon nanotubes as energy conversion materials to fabricate thin-film solar cells, with nanotubes serving as both photogeneration sites and a charge carriers collecting/transport layer. The solar cells consist of a semitransparent thin film of nanotubes conformally coated on a n-type crystalline silicon substrate to create high-density p–n heterojunctions between nanotubes and n-Si to favor charge separation and extract electrons (through n-Si) and holes (through nanotubes). Initial tests have shown a power conversion efficiency of >1%, proving that DWNTs-on-Si is a potentially suitable configuration for making solar cells. Our devices are distinct from previously reported organic solar cells based on blends of polymers and nanomaterials, where conjugate polymers generate excitons and nanotubes only serve as a transport path.

**Introduction.** Previous use of carbon nanotubes in organic solar cell applications was mainly confined as nanoscale fillers (providing transport path) to polymer matrix or as transparent electrodes for collecting charge carriers.<sup>1–8</sup> It was believed that the high aspect ratios and large surface area of nanotubes could be beneficial to exciton dissociation and charge carrier transport thus improves the power conversion efficiency. However, donor–acceptor (D–A) type structures consisting of conjugated polymers such as poly(3-hexylthiophene) (P3HT) or poly(3-octylthiophene) (P3OT) mixed with nanotubes have shown negligible efficiency (<0.1%), even with the addition of dye.<sup>9</sup> After appropriate postannealing treatment, the efficiency is only about 0.22%.<sup>10</sup> Further, the challenge of nanotube dispersion in polymers and separating semiconducting tubes from metallic species plus the very low hole mobilities of polymers, typically below  $10^{-4} \text{ cm}^2 \text{ V}^{-1} \text{ s}^{-1}$  (<0.1  $\text{cm}^2 \text{ V}^{-1} \text{ s}^{-1}$  for P3HT), are all limiting factors to the device fabrication and performance. In addition, nanotube films (by spin-cast or direct growth) used as transparent electrodes have shown negligible improvement of efficiency compared with ITO glass.<sup>5–7</sup>

In those reports, nanotubes do not participate in photogeneration process; it is the conjugated polymers (e.g., P3HT)

that produce excitons under optical excitation. Nanotubes, when embedded into the polymer matrix, only provide more interfacial area for exciton dissociation and charge transport path. Nonetheless, theoretical study has predicted photoconductivity of individual nanotubes,<sup>11,12</sup> and appreciable photocurrent has been observed when nanotube films were irradiated by light.<sup>13,14</sup> We have demonstrated that macrosized bundles consisting of double-walled nanotubes (DWNTs) could generate photocurrent at an energy conversion efficiency of up to 0.5% under illumination of light in the visible region.<sup>15,16</sup>

Here, we directly use DWNTs as the energy conversion material to construct thin-film solar cells and remove the use of polymers. The DWNTs serve as photogeneration sites as well as a ballistic transport path for charge carriers (holes), and a piece of n-type silicon wafer was used to extract electrons. While most of work has primarily focused on single-walled or multiwalled nanotubes, DWNTs have been seldom introduced to solar cells<sup>17</sup> even though they have advantages such as possessing similar diameter with single-walled tubes but with higher stability. Initial tests have shown a power conversion efficiency of >1%, and we attribute these promising results to the photoconductivity and high mobility ( $>10^5 \text{ cm}^2 \text{ V}^{-1} \text{ s}^{-1}$ )<sup>18</sup> of nanotubes.

**Experimental.** We have made macroscopic DWNT films ( $>100 \text{ cm}^2$ ) with controlled thickness by an improved chemical vapor deposition method.<sup>19,20</sup> The as-grown DWNT films were treated in  $\text{H}_2\text{O}_2$  and HCl solution and rinsed with

\* Corresponding authors. E-mail: jqwei@mail.tsinghua.edu.cn (J.W.); wdh-dme@tsinghua.edu.cn (D.W.). Telephone: +86-10-62792846. Fax: +86-10-62770190.

<sup>†</sup> Key Lab for Advanced Manufacturing by Materials Processing Technology of Education Ministry, Department of Mechanical Engineering, Tsinghua University.

<sup>‡</sup> Department of Mechanical Engineering, University of Hawaii at Manoa.

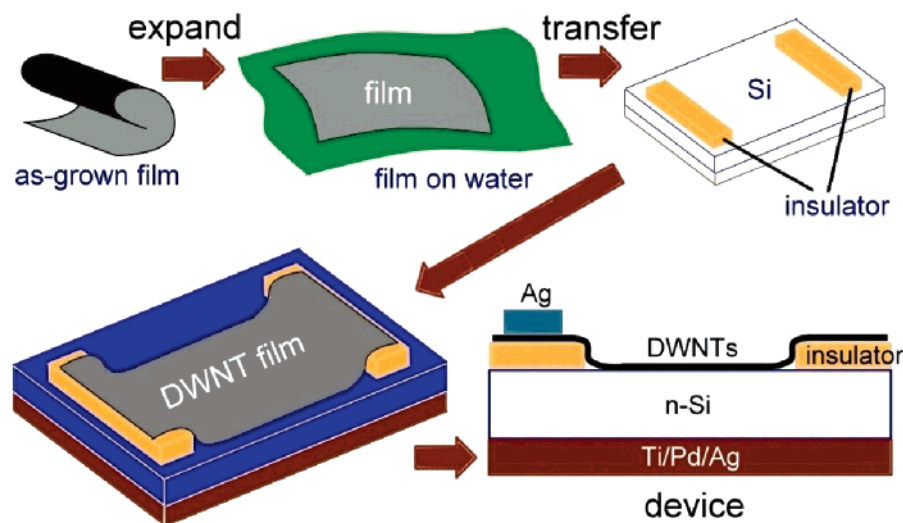


**Figure 1.** Illustration of the fabrication process of DWNT/n-Si solar cell. The as-grown DWNT films were fully expanded in a water solution and then conformally transferred to a patterned Si substrate.

distilled water to pH = 7 to remove the impurities of catalytic particles and amorphous carbon. The DWNTs were suspended in distilled water, and by adding a few drops of ethanol on top of the film, they fully expanded into an ultrathin flat film floating on the water surface. A piece of n-type silicon (n-Si) wafer with a window of predeposited insulating layer was immersed into water to pick up the expanded film, as illustrated in Figure 1. The DWNT films were conformally transferred to the Si wafer with excellent adhesion to the wafer surface after drying at room temperature; flushing the film with water did not detach it from substrate. The DWNT films were characterized by scanning electronic microscope (SEM), high-resolution transmission electronic microscope (HRTEM), and UV–visible spectra.

The solar cell was constructed by conformally coating a transparent DWNT film onto a n-type bulk crystalline silicon substrate (thickness 525  $\mu\text{m}$ ) with a window of  $7 \times 7 \text{ mm}^2$  surrounded by an insulating isinglass sheet (Figure 1). The upper electrode connects to the DWNT film by silver paint (separated from the underlying Si by isinglass insulator). A Ti/Pd/Ag layer (thickness  $\sim 2 \mu\text{m}$ ) was sputtered at the back side of Si substrate as the bottom electrode. Forward bias is defined as positive voltage applied to the DWNT film. To perform the testing, the devices were irradiated under a solar simulator (Thermo Oriel 91192-1000) at AM1.5, and data were recorded using a Keithley 4200.

**Results and Discussion.** SEM characterization reveals a porous network structure of the as-coated DWNT film that is virtually free of catalyst residue or amorphous carbon particles (Figure 2a). The DWNTs lying on the substrate surface form numerous heterojunctions in contact with the underlying n-Si. The DWNT bundles occupy about 25% of the total film area calculated from tens of SEM images by graphic analyzer. The DWNTs have an outer diameter of 2–2.5 nm and usually are arranged in 20–50 nm diameter bundles from HRTEM characterization (Figure 2b). Cross-sectional view shows uniform film thickness ( $\sim 50 \text{ nm}$ ) and good contact between DWNT bundles and the Si substrate (Figure 2c). This fully expanded film, consisting of a few

DWNT layers, is about 50–100 nm in thickness over centimeter area. The film thickness can be further controlled to reach hundreds of nanometers by overlapping multiple layers through repeated conformal transfer as described in Figure 1.

DWNT films were also collected by transparent quartz glass to investigate the optical property. Films with thicknesses of 35 or 55 nm show a transmission of  $> 60\%$  in the visible light region. The transmissions at a wavelength of 550 nm remain above 40% for films with larger thicknesses (e.g., 200 nm) (Figure 2d). Such semitransparency ensures the absorption of the solar light by both the DWNT film and the underlying Si. Our DWNT samples are a complex of conductive and semiconductive type of CNTs. Four-probe measurements show that sheet resistances varies from 0.5  $\Omega/\text{sq}$  to 5  $\Omega/\text{sq}$  for DWNT films with thicknesses of 35–200 nm, which is lower than that of the ITO ( $\sim 15 \Omega/\text{sq}$ ). Thus, our DWNT films can be directly used as a transparent conductive layer for solar cells, which can simplify the fabricating process of the CNT solar cell.

Figure 3a shows the  $I$ – $V$  characteristics of a typical DWNT/n-Si solar cell, in which the DWNT film is about 50 nm in thickness, in dark and under white light illumination (AM1.5, 100  $\text{mW}/\text{cm}^2$ ). The device shows an evident p–n junction behavior in the dark, where the reversed current density is very low ( $\sim 30 \mu\text{A}/\text{cm}^2$ , over 500 times lower than the forward current density) when the bias voltage sweeps from  $-2.0$  to  $0 \text{ V}$  compared to forward current ( $\sim 16 \text{ mA}/\text{cm}^2$  at  $1.0 \text{ V}$ ) as shown in Figure 3a. Under illumination, the  $I$ – $V$  curve shifts downward, with an open-circuit voltage  $V_{\text{oc}}$  and short-circuit current density  $J_{\text{sc}}$  of about 0.5 V and 13.8  $\text{mA}/\text{cm}^2$ , respectively. Measurements on 10 solar cells composed of DWNT films at similar thickness (50–100 nm) synthesized from different CVD batches (same growth condition) show a reasonable reproducibility of  $V_{\text{oc}}$  and  $J_{\text{sc}}$ , although fluctuations ( $V_{\text{oc}}$  within the range of 0.35–0.55 V and  $J_{\text{sc}}$  within the range of 5–15  $\text{mA}/\text{cm}^2$ ) were observed from device to device. While the value of  $V_{\text{oc}}$  is comparable to previous reports based on P3HT–DWNT composite

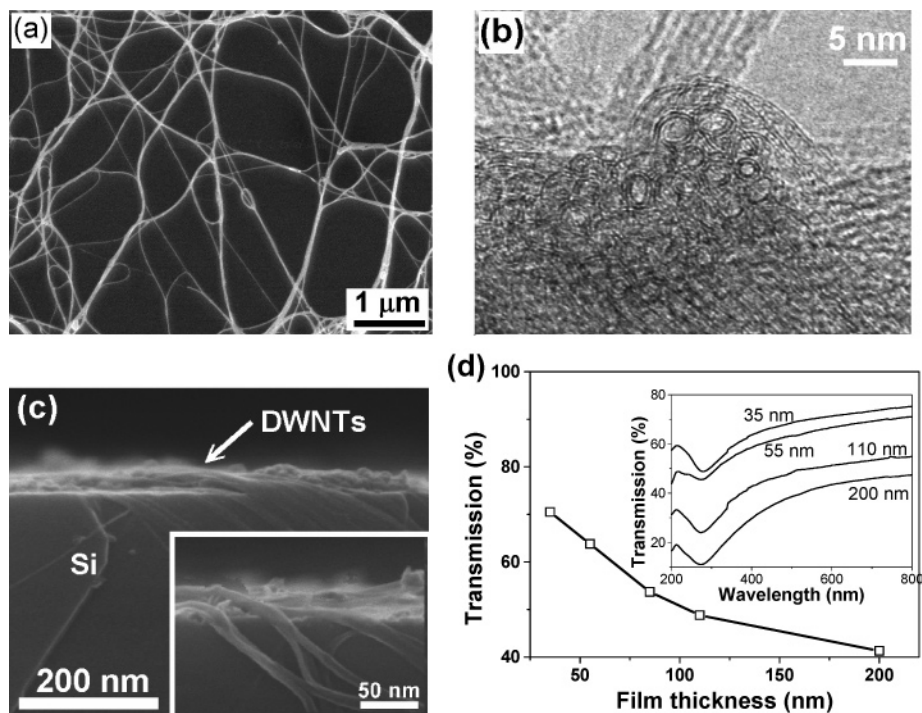


**Figure 2.** Characterization of DWNT films. (a) SEM image of a DWNT film showing porous network structure. (b) HRTEM image of DWNTs revealing double-walled structure. (c) Cross-sectional SEM image of DWNT film transferred to the top of Si substrate. Inset: DWNT bundles in close contact to the Si surface. (d) Optical transmission (at 550 nm) of DWNT films with different thicknesses. Inset: Transmission of DWNT films in visible region.

structures, the  $J_{sc}$  of this DWNT/n-Si solar cell without polymer (P3HT) addition has been enhanced over 40 times more than that of the composite cells ( $0.34 \text{ mA/cm}^2$ ).<sup>17</sup>

The fill factor (FF) and power efficiency ( $\eta$ ) of the DWNT/n-Si solar cell are about 19% and 1.38%, respectively (Figure 3a). Compared with previous solar cell configurations based on conjugated polymers mixed with single-walled nanotubes (SWNTs) or DWNTs (FF = 15–30%,  $\eta \ll 1\%$ ),<sup>1,4,9,10,17</sup> our devices show a fill factor in similar range but much higher efficiency. And we believe our devices have the potential to be further optimized, for example, by tailoring the density and thickness of DWNT films, so that they achieve much improved power conversion efficiency. Although there are both semiconducting and metallic tubes in the film, the shorting of the device does not occur, as seen from the p–n junction property. We have sputtered a few gold lines between the DWNT film and n-Si to create a shorting path in the solar cell, and the current density has decreased over 50 times.

We found that the photoinduced current is very weak ( $<1 \mu\text{A/cm}^2$ ) when solar light irradiates only DWNT films without the presence of n-Si substrate, indicating that a significant value of  $V_{oc}$  and  $J_{sc}$  of the DWNT solar cells originates from the creation of heterojunctions at the interface between the DWNT film and the n-Si. Although having similar diameter to SWNTs, which usually behave as p-type semiconductors, the DWNTs have shown ambipolar (both p- and n-type) conducting behavior, presumably owing to smaller band gaps according to previous reports.<sup>21</sup> It indicates that there could be large amount of holes available in DWNTs, which is consistent with early study on field effect

transistors of carbon nanotubes.<sup>22</sup> When fully expanded on a planar Si substrate, there will be numerous p–n junctions formed due to close contact between DWNTs and underlying n-Si. The  $I$ – $V$  curve in the dark actually shows a typical diode behavior, further confirming the existence of p–n junction of this DWNTs-on-Si configuration (Figure 3a).

In our previous work, when a bundle of nanotubes was brought into contact with a macroscopic metal electrode to form a nanotube/metal heterojunction, evident photocurrent can be detected.<sup>16</sup> The high  $J_{sc}$  of the DWNT solar cells indicates that the generation/transport of charge carriers from both DWNTs and silicon when irradiated by solar light has been enhanced dramatically due to the presence of high density p–n junctions. Pasquier's work shows that nanotubes act mainly as hole collectors and conductors in polymer–nanotube solar cells.<sup>23</sup> However, we believe that, in our situation, DWNTs have participated in the photogeneration process as well as charge transport, and their high mobility ensures much enhanced efficiency compared with polymer composite cell structures.

At forward bias ( $V > V_{oc}$ ), it can be seen that the current density in the dark (without irradiation) is much higher than the value measured under solar light, indicating light irradiation causes dropping of current at this voltage range (Figure 3a). This result is consistent with observed current reduction for DWNT bundles under light irradiation,<sup>15</sup> although in contrast to previous observation on polymer–nanotube systems where light illumination increases the current density at  $V > V_{oc}$ .<sup>1,4</sup> Our previous reports have demonstrated the photoinduced current flow through DWNT

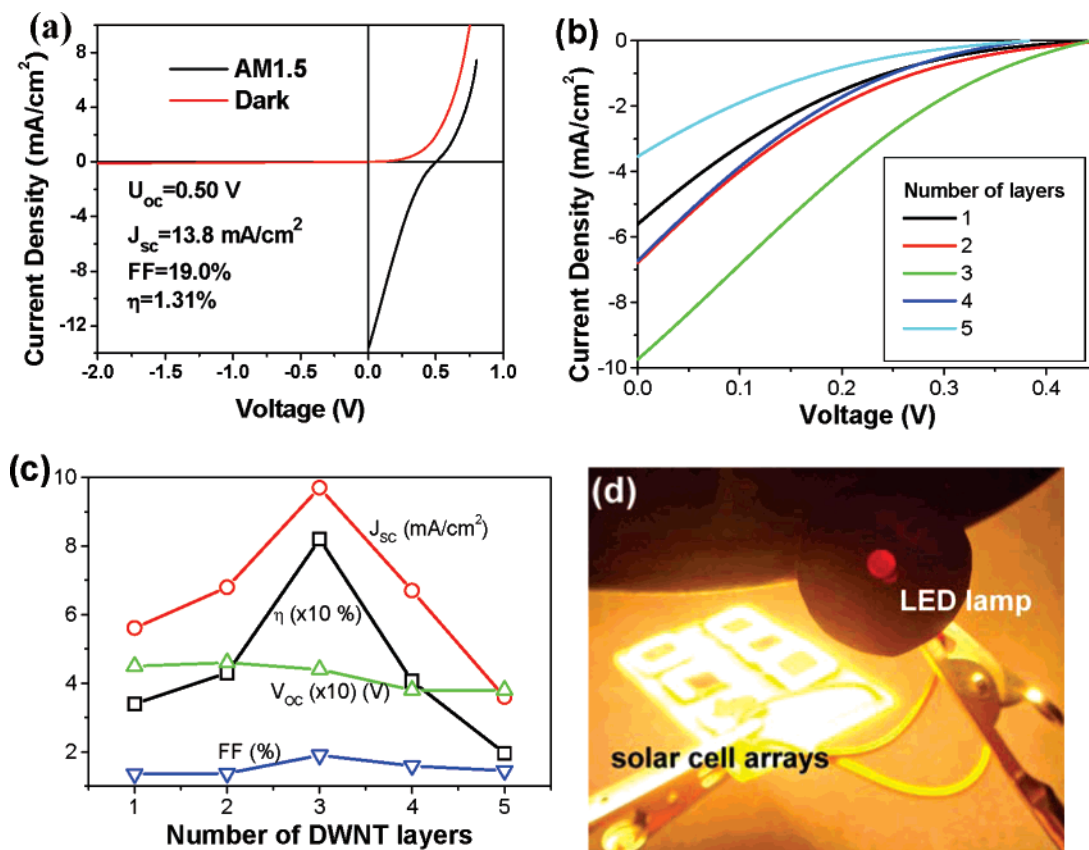


**Figure 3.** Device characterization. (a) Current–voltage plot of a typical DWNT/n-Si device in dark and under illumination, showing typical solar cell performance with efficiency of 1.3%. (b) Current–voltage plots of solar cells consisting of multiple overlapped DWNT layers (from one to five layers). (c) Summary of short-circuit current ( $J_{sc}$ ), open-circuit voltage ( $V_{oc}$ ), fill factor (FF), and efficiency ( $\eta$ ) for DWNT cells with multiple layers, showing maximum current and efficiency of the triple-layer device. (d) A LED lamp (red) lighted by six DWNT solar cells connected in series supplying a total voltage of 1.8 V irradiated by a room light (40 W).

bundles under illumination at the visible region,<sup>15,16</sup> and the current could be enhanced when light illuminates on the interface between the DWNTs and metal electrode (reaching about  $0.2 \text{ mA/cm}^2$  for an laser intensity of about  $100 \text{ mW/cm}^2$  at  $780 \text{ nm}$ )<sup>16</sup>. Now for our configuration where DWNTs lay on the Si substrate, the  $J_{sc}$  actually reaches  $13.8 \text{ mA/cm}^2$  at  $100 \text{ mW/cm}^2$  light intensity, about 70 times higher than that of the DWNT–metal junction. It may due to the fact that the photoinduced electrons are injected to n-type Si while holes are transported through p-type DWNTs more efficiently, given the much larger interfacial area created by a fully expanded film compared with a thick bundle where the DWNTs well within the bundle do not contact directly the metal electrodes. A Schottky junction made by sputtering a gold grid (to replace the DWNT film) on top of Si did produce some power conversion, but the current density is 2–3 orders of magnitude lower (about several  $\mu\text{A/cm}^2$ ) than the DWNT–Si junction.

We found that the series resistance of the device mainly comes from the electrical contact to the bottom of n-Si substrate. By depositing a Ti/Pd/Ag layer with good adhesion to Si, the  $J_{sc}$  has been enhanced by a factor of 10 compared with the use of silver paint as contact. Currently, the series resistance calculated from the dark  $I$ – $V$  characteristics is about  $30$ – $200 \text{ }\Omega$ , which could be further reduced by decreasing the Si substrate thickness or improving the

fabrication process (such as using a  $\text{SiO}_2$  thin film depositing on the silicon wafer to replace the isinglass sheet or improving the contact between the CNTs and the upper electrode) of DWNT/Si solar cells.

The flexibility of the fabrication process allows us to construct cell devices containing multiple DWNT films by repeating the solution transfer process. We have made cells with tailored thicknesses from  $35$  to about  $250 \text{ nm}$  by overlapping one–five layers of uniform DWNT films. All the cells show relatively stable voltages ( $V_{oc}$ ) ranging from  $0.4$  to  $0.45 \text{ V}$ , but quite different current densities ( $J_{sc}$ ) (Figure 3b). The cell with three layers (thickness of  $\sim 120 \text{ nm}$ ) shows the highest  $J_{sc}$  ( $9.7 \text{ mA/cm}^2$ ) and  $\eta$  ( $0.82\%$ ), over two times larger than those of the single-layer cell (Figure 3c). At further increased thickness (five layers), the values of  $J_{sc}$  and  $\eta$  decrease significantly (Figure 3c). Overlapping multiple layers increases both the density of DWNTs and the total area of DWNT–Si junctions in the device, which could enhance the current generation/transport. However, at above four layers (about  $200 \text{ nm}$  in thickness), the DWNTs at top layers are suspending on the underneath layers and cannot touch the Si substrate to form junctions. Also, thicker films are less transparent and preventing more incident light from reaching the substrate. Our results show an optimal thickness of DWNT films of about  $100$ – $150 \text{ nm}$ , with maximum current density and efficiency.

Figure 3d shows a photo of an array of six solar cells connected in series (3 cells by 2 rows), which lights up a LED light when the cells are illuminated with a room light with a rated power of 40 W. The total voltage of the array reaches about 1.8 V when it is illuminated by room light, with an average value of about 0.3 V being supplied by each cell. The turning on of the LED light is instantaneous upon illumination of connected solar cells. We have observed a stable LED lighting for over 100 h without obvious degradation of the output voltage from this cell array. The total working area (DWNT film) of the array is only 3 cm<sup>2</sup>, which shows that the nanotube solar cells may be easily integrated into portable light sources or signal lamps for use at the cross-sections of roads.

**Conclusion.** Our results have shown that carbon nanotubes can be directly used as the energy conversion materials in solar cells, serving for both the photogeneration process and charge carrier transport. The numerous heterojunctions formed between p-DWNTs and n-Si perform just as the conventional p–n junctions in the generation of electron–hole pairs, which are then split and transported through DWNTs (holes) and n-Si (electrons), respectively. The large carrier density and high mobility of DWNTs ensure much enhanced current density and power efficiency of solar cells compared with extensively studied polymer–nanotube composite structures. While initial results are based on Si, we believe the concept also applies to other cheaper or flexible thin-film substrates in the future research for low-cost production.

**Acknowledgment.** This work is supported by National Natural Science Foundation (Grand No. 50672047) and Chinese National Center for Nanoscience and Technology.

## References

- (1) Kymakis, E.; Amaratunga, G. A. J. *Appl. Phys. Lett.* **2002**, *80*, 112–114.
- (2) Landi, B. J.; Raffaele, R. P.; Castro, S. L.; Bailey, S. G. *Prog. Photovoltaics: Res. Appl.* **2005**, *13*, 165–172.
- (3) Brabec, C. J.; Sariciftci, B. N. S.; Hummelen, J. C. *Adv. Funct. Mater.* **2001**, *11*, 15–26.
- (4) Pradhan, B.; Batabyal, S. K.; Pal, A. J. *Appl. Phys. Lett.* **2006**, *88*, 093106–093108.
- (5) van de Lagemaat, J.; Barnes, T. M.; Rumbles, G.; Shaheen, S. E.; Coutts, T. J.; Weeks, C.; Levitsky, I.; Peltola, J.; Glatkowski, P. *Appl. Phys. Lett.* **2006**, *88*, 233503.
- (6) Rowell, M. W.; Topinka, M. A.; McGehee, M. D.; Prall, H. J.; Dennler, G.; Sariciftci, N. S.; Hu, L. B.; Gruner, G. *Appl. Phys. Lett.* **2006**, *88*, 233506.
- (7) Miller, A. J.; Hatton, R. A.; Chen, G. Y.; Silva, S. R. P. *Appl. Phys. Lett.* **2007**, *90*, 023105–023107.
- (8) Ago, H.; Petritsch, K.; Shaffer, M. S. P.; Windle, A. H.; Friend, R. H. *Adv. Mater.* **1999**, *11*, 1281–1285.
- (9) Bhattacharyya, S.; Kymakis, E.; Amaratunga, G. A. J. *Chem. Mater.* **2004**, *16*, 4819–4823.
- (10) Kymakis, E.; Koudoumas, E.; Franghiadakis, I.; Amaratunga, G. A. J. *J. Phys. D: Appl. Phys.* **2006**, *39*, 1058–1062.
- (11) Freitag, M.; Martin, Y.; Misewich, J. A.; Martel, R.; Avouris, P. H. *Nano Lett.* **2003**, *3*, 1067–1071.
- (12) Stewart, D. A.; Léonard, F. *Phys. Rev. Lett.* **2004**, *93*, 107401.
- (13) Lu, S. X.; Panchapakesan, B. *Nanotechnology* **2006**, *17*, 1843–1850.
- (14) Fujiwara, A.; Matsuoka, Y.; Suematsu, H.; Ogawa, N.; Miyano, K.; Kataura, H.; Maniwa, Y.; Suzuki, S.; Achiba, Y. *Jpn. J. Appl. Phys.* **2001**, *40*, L1229–L1231.
- (15) Wei, J. Q.; Sun, J. L.; Zhu, J. L.; Wang, K. L.; Wang, Z. C.; Luo, J. B.; Wu, D. H.; Cao, A. Y. *Small* **2006**, *2*, 988–993.
- (16) Sun, J. L.; Wei, J. Q.; Zhu, J. L.; Xu, D.; Liu, X.; Sun, H.; Wu, D. H.; Wu, N. L. *Appl. Phys. Lett.* **2006**, *88*, 131107–131109.
- (17) Somani, S. P.; Somani, P. R.; Umeno, M.; Flahaut, E. *Appl. Phys. Lett.* **2006**, *89*, 223505.
- (18) Dürkop, T.; Getty, S. A.; Cobas, E.; Fuhrer, M. S. *Nano Lett.* **2004**, *4*, 35–39.
- (19) Wei, J. Q.; Zhu, H. W.; Li, Y. H.; Chen, B.; Jia, Y.; Wang, K. L.; Wang, Z. C.; Liu, W. J.; Luo, J. B.; Zheng, M. X.; Wu, D. H.; Zhu, Y. Q.; Wei, B. Q. *Adv. Mater.* **2006**, *18*, 1695–1700.
- (20) Wei, J. Q.; Jiang, B.; Wu, D. H.; Wei, B. Q. *J. Phys. Chem. B* **2004**, *108*, 8844–8847.
- (21) Shimada, T.; Sugai, T.; Ohno, Y.; Kishimoto, S.; Mizutani, T.; Yoshida, H.; Okazaki, T.; Shinohara, H. *Appl. Phys. Lett.* **2004**, *84*, 2412–2414.
- (22) Martel, R.; Schmidt, T.; Shea, H. R.; Hertel, T.; Avouris, P. *Appl. Phys. Lett.* **1998**, *73*, 2447–2449.
- (23) Pasquier, A. D.; Unalan, H. E.; Kanwal, A.; Miller, S.; Chhowalla, M. *Appl. Phys. Lett.* **2005**, *87*, 203511.

NL070961C